

# Oxidation-Responsive Micelles for Drug Release Monitoring and Bioimaging of Inflammation Based on FRET Effect in vitro and in vivo

Ziqiang Zhou<sup>1</sup>, Yanfang Wang<sup>2</sup>, Ping Hu<sup>1</sup>

<sup>1</sup>College of Pharmacy, Jinan University, Guangzhou, People's Republic of China; <sup>2</sup>First Affiliated Hospital of the Medical College, Shihezi University, Shihezi, People's Republic of China

Correspondence: Ping Hu, College of Pharmacy, Jinan University, No. 855, East Xingye Avenue, Panyu District, Guangzhou, 511436, People's Republic of China, Tel +86-18581483142, Email [inzahu@hotmail.com](mailto:inzahu@hotmail.com)

**Purpose:** A new approach to monitor drug release and image inflammatory reactions in vitro and in vivo based on FRET mechanism was reported.

**Methods:** In this study, mixed micelles containing a synthesized fluorescent donor DAN-PPS-mPEG and its quencher DAB-PPS-mPEG were prepared. Their stabilities, self-assembling and oxidation-responsiveness towards oxidants were tested in vitro and in vivo.

**Results:** The conjugated polymers were synthesized and the morphological change and the fluorescent spectra of the prepared micellar system were measured. After incubating the DAN/DAB-PPS-mPEG mixed micelles with stimulated L929 fibroblast cells, the result of confocal laser microscopy showed fluorescence restoration of the micelles. Furthermore, an acute inflammatory injury mouse model was used to test the micelles in vivo. The micelles showed its ability to visualize the inflammatory site in the abdomen of the mice.

**Conclusion:** The results confirmed that DAN/DAB-PPS-mPEG mixed micelles can respond to oxidants and release encapsulated cargos with corresponding fluorescence restoration, and visualize the inflammatory cells in vitro and inflammatory reactions in vivo.

**Keywords:** FRET, ROS, micelles, oxidation responsiveness

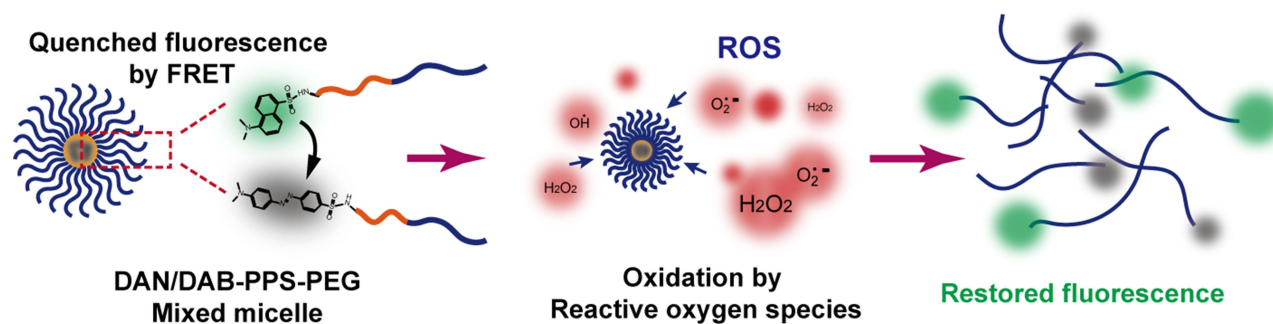
## Introduction

Reactive oxygen species (ROS) are extensively related to multiple biological processes.<sup>1,2</sup> As pro-oxidants, reactive oxygen species (ROS) are the by-products of aerobic metabolism in the body and mainly include hydroxyl radicals (OH<sup>•</sup>), superoxide anions (O<sub>2</sub><sup>•-</sup>), nitrites (ONOO<sup>-</sup>), and hydrogen peroxide (H<sub>2</sub>O<sub>2</sub>). ROS can act as a mediator of a variety of cellular signal transduction during the normal physiological conditions, including regulating cell growth and stress adaptation.<sup>3,4</sup> Conversely, the body produces excess ROS when it suffers from surgery or diseases, such as cancer, cardiovascular disease, diabetes and neurological decomposition diseases, etc., mostly due to the formation and development of inflammation.<sup>5-7</sup>

Numerous drug molecules and delivery systems targeting inflammation have been developed in recent years to either directly act on the inflammatory cells, or responsively release therapeutic cargos upon interacting with the inflammatory biomarkers such as ROS.<sup>8-11</sup> These drug delivery systems (DDS), typically consisting of thioether-containing polymers,<sup>12,13</sup> selenium-containing polymers and phenylboronic acid /phenylboronic ester-containing polymers etc.,<sup>14,15</sup> called as oxidation-responsive DDS. They are capable of responding to cell generated oxygen species and represent a promising methodology because of their potential in ROS sensing and elimination, precise drug and gene delivery, as well as cell protection against oxidative stress.<sup>8</sup>

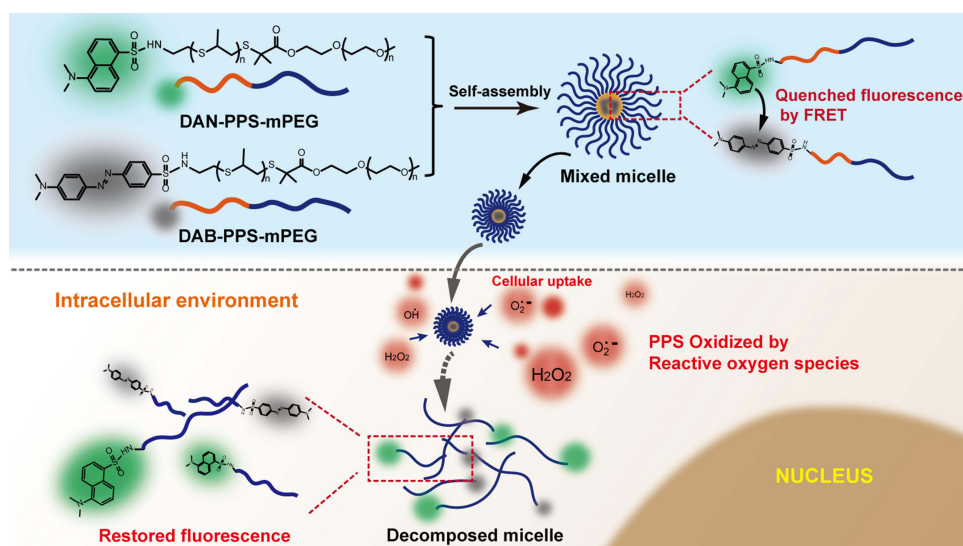
With the advance in medical therapy, the treatment integrated with diagnosis and therapy has become more and more popular. It will be highly beneficial to treat a certain disease and at the same time visualize the treatment site and monitor the recovery process. Fluorescent probes are commonly used and have been proven to be effective tools to monitor

## Graphical Abstract



biologically relevant species *in vivo* due to their numerous advantages, such as high sensitivity, simple manipulation, excellent temporal-spatial resolution, real-time spatial imaging, etc.<sup>16</sup> A number of fluorescent probes for ROS detection *in vivo* have been reported.<sup>17,18</sup> However, using these probes can only report the location of the ROS, additional therapeutic drugs or drug carriers are still needed to travel to the site with the presence of excessive ROS to play their therapeutic roles, which are two separated processes.

In this study, we developed a novel oxidation-responsive polymeric micellar system, which can simultaneously absorb ROS and release encapsulated cargos, as well as generate fluorescent signal to reflect the drug release and visualize the presence of ROS (Scheme 1). The ROS triggered the generation of fluorescence and the intensity of the generated fluorescence is related to the progress of micellar decomposition and the extent of drug release. As shown in Scheme 1, we firstly synthesized an amphiphilic diblock copolymer PPS-mPEG via a living anionic polymerization process.<sup>19,20</sup> Polypropylene sulfide (PPS) is a type of well-studied hydrophobic oxidation-responsive polymer, which can consume intracellular ROS and transformed to more hydrophilic polypropylene sulfoxide or sulfone due to the oxidation of the sulfur atoms on the polymer backbone.<sup>12,21</sup> Dansyl and dabsyl groups were conjugated to the amino groups of the polymer to form a fluorescent donor DAN-PPS-mPEG and its quencher DAB-PPS-mPEG.<sup>22</sup> After preparing a mixed micelle using these two paired polymers, the self-assembled polymeric micelle showed a quenched fluorescence state via fluorescence resonance energy transfer (FRET) principle between the dansyl and dabsyl groups. FRET is a nonradiative process whereby an excited state donor (usually a fluorophore) transfers



**Scheme 1** The illustration of the self-assembling of the DAN/DAB-PPS-mPEG micelles and their fluorescent restoration upon oxidation in the inflammatory cells.

energy to a proximal ground state acceptor through long-range dipole–dipole interactions.<sup>23</sup> The acceptor must absorb energy at the emission wavelength of the donor but does not necessarily have to remit the energy fluorescently itself. The rate of energy transfer is highly relied on many factors, such as the extent of spectral overlap, and the distance between the donor and acceptor molecules is the most important factor to consider.<sup>24</sup> In the presence of ROS, the mixed micelle will undergo an oxidation process of the PPS block and decompose to release the quenched fluorescence, due to the increased distance between the fluorescent donor and acceptor. The restoration of the fluorescence of the micelles was correlated with the decomposition of the micelles and the drug release process in vitro, using Nile Red as a model hydrophobic drug. Moreover, in vitro and in vivo bioimaging experiments of demonstrated that DAN/DAB-PPS-mPEG mixed micelle facilitated the visualization of endogenous ROS in an inflammatory cell model and in a LPS induced acute inflammation injury mouse model.

## Materials and Methods

### Materials

tris-n-butylphosphine (TBP, >99%), 1,8-diazabicyclo[5.4.0] undec-7-ene (DBU, 98%), Acetic acid (ACA, >99.5%), Sodium methoxide (Ca. 5 mol/L in methanol), Tetrahydrofuran (THF), trifluoroacetic acid (TFA) were purchased in Energy chemical company (Shanghai, China). Propylene sulfide (PS, 98%), Nile Red (98%), dansyl chloride (>99%), dabsyl chloride (>99%), hydrogen peroxide (H<sub>2</sub>O<sub>2</sub>) were purchased from Sigma (St. Louis, USA). Rosup was purchased from Beyotime Institute of Biotechnology (Beijing, China). L929 cell line was purchased from the Culture Collections of the Chinese Academy of Science (Shanghai, China). Nude mice was purchased from the animal center of the Chinese Academy of Science (Shanghai, China).

### Polymers Synthesis and Characterizations

A Boc protected thiol initiator was synthesized according to published procedure.<sup>21</sup> In a general procedure, the initiator (2.02 mmol) stock solution and tributyl phosphate (TBP, 5.0 equiv.) in 5 mL of degassed THF were transferred to a reactor. The mixture was stirred at room temperature for 5 min followed by adding 10 equiv. of propylene sulfide (PS) to the mixture and allowed to react for 45 min. End-capping agent (0.95 equiv. of ethyl 2-bromoacetate mPEG) was finally added and the mixture was stirred for 2 h at room temperature. After removing the solvent with a rotary evaporator, the PPS-mPEG was obtained by precipitation in ice-cold diethyl ether twice and dried at room temperature under vacuum. Obtained PPS-mPEG (0.29 mmol) was dissolved in 15 mL of anhydrous THF followed by addition of TFA (55  $\mu$ L, 0.39 mmol) under nitrogen atmospheres to remove the Boc and expose the terminal amine group. The reactant mixture was concentrated and precipitated in ice-cold diethyl ether again to afford the intermediate polymer NH<sub>2</sub>-PPS-mPEG. Dansyl chloride or dabsyl chloride (0.2 mmol) and 0.5 mmol of TEA was dissolved in 10 mL of THF, followed by the addition of 0.15 mmol of synthesized polymer. After 24 hours of reaction, the resulting polymers were treated and purified using the same procedures as described to afford the final products DAN-PPS-mPEG and DAB-PPS-mPEG. The final product was dried under vacuum.

<sup>1</sup>H-NMR (CDCl<sub>3</sub>): DAN-PPS-mPEG: 1.35–1.45 (d, CH<sub>3</sub> in PPS chain), 1.48–1.58 (s, 6H, -C(CH<sub>3</sub>)<sub>2</sub>), 2.55–2.70 (m, 1 diastereotopic H of CH<sub>2</sub> in PPS chain), 2.85–3.05 (m, CH and 1 diastereotopic H of CH<sub>2</sub> in PPS chain), 3.15 (s, 3H, -N(CH<sub>3</sub>)<sub>2</sub>), 3.40 (s, 3H, -OCH<sub>3</sub>), 3.6–3.8 (broad, PEG chain protons), 7.48 (d, 1H, aromatic CH ortho to aniline), 7.55–7.65 (dt, 2H, aromatic CH meta to aniline and meta to sulfone group), 8.38–8.48 (dd, 2H, aromatic CH para to aniline and para to sulfone group), 8.66 (d, 1H, aromatic CH ortho to sulfone group) ppm.

DAB-PPS-mPEG: 1.35–1.45 (d, CH<sub>3</sub> in PPS chain), 1.52–1.62 (s, 6H, -C(CH<sub>3</sub>)<sub>2</sub>), 2.55–2.70 (m, 1 diastereotopic H of CH<sub>2</sub> in PPS chain), 2.80–2.95 (m, CH and 1 diastereotopic H of CH<sub>2</sub> in PPS chain), 3.15 (s, 3H, -N(CH<sub>3</sub>)<sub>2</sub>), 3.40 (s, 3H, -OCH<sub>3</sub>), 3.6–3.75 (broad, PEG chain protons), 6.78 (d, 2H, aromatic CH ortho to aniline), 7.85–7.95 (m, 4H, aromatic CH ortho to azo group), 8.05 (d, 2H, aromatic CH ortho to sulfone group) ppm.

<sup>1</sup>H-NMR spectra were obtained on a Bruker Avance 400 instrument. Gel permeation chromatography (GPC) was measured by using an Agilent GPC equipped with a 1260 Infinity Isocratic Pump and a RI detector. Two Agilent PL gel mixed-E columns were used with DMF as the mobile phase at 30 °C (1.0 mL/min).

## Preparation of DAN/DAB-PPS-mPEG Micelles

DAN/DAB-PPS-mPEG micelles were prepared by dissolving 10 mg of mixed polymer in 1 mL of THF, followed by injecting the organic solution into 10 mL of double distilled water and stirred at room temperature for 20 min. The organic solvent was removed by a rotary evaporator (80 mbar for 30 min,  $T = 25^{\circ}\text{C}$ ). Different micelles with different ratio of DAN/DAB-PPS-mPEG polymers (1:1, 1:2, 1:3, 1:4) were prepared to find out a suitable ratio of the fluorescent donor and quencher. Nile Red labeled DAN-PPS-mPEG micelle or mixed micelle (the ratio of DAN/DAB conjugated polymers is 1:3) was prepared. 0.1 mg of Nile Red was added to the THF solution of polymers, and the micelles were prepared followed the same procedure as the blank micelles.

## Characterizations of the Micelles

The size distributions of the DAN/DAB-PPS-mPEG micelles and Nile Red loaded micelles were measured using a Malvern Instruments Nano ZS90 equipped with a 633 nm He-Ne gas laser. The micelles were imaged using a Tescan MIRA 3 LMH scanning electron microscope (SEM). The micellar dispersion was suspended in water, deposited on silicon wafers and left to dry overnight and imaged. Additionally, the fluorescence intensities of the micelles dispersions prepared with DAN-PPS-mPEG mixed with different amount of  $\text{NH}_2$ -PPS-mPEG (1 mg/mL) were recorded to test the possible self-quenching effect of the dansyl fluorophore.

## Oxidation-Responsiveness of the Micelles

The fluorescence of the blank micelle and Nile Red loaded micelle upon oxidation was measured and recorded using a fluorescence spectrophotometer (Hitachi F-7000 FL Spectrophotometer). 500  $\mu\text{L}$  of Nile Red loaded (DAN/DAB = 1:3) mixed micelle (1 mg/mL) was placed in a cuvette, which contains 2 mL of 0.5%  $\text{H}_2\text{O}_2$  release media. At different time point, the fluorescence spectra of the sample were measured using different excitation wavelengths (Dansyl excitation wavelength at 335 nm, Nile Red excitation wavelength at 560 nm) with the fluorescence spectrophotometer.

The change of the scattering intensity of the mixed micelles was also measured. The sample was prepared using the same procedure described above. 1 mL of the sample mixed with micelles and 0.5%  $\text{H}_2\text{O}_2$  (V/V = 1:4) was put into the chamber of the above mentioned Nanosizer. The scattering intensities of the sample were measured and recorded at different time points.

The physiological stability of the prepared mixed micelles were evaluated by measuring the relative scattering intensities of the mixed micelles incubated in water, PBS, 0.5%  $\text{H}_2\text{O}_2$  and rat plasma for 24 h.

## Confocal Imaging of Cells

Mouse fibroblast cells (L929 cell line) were cultured in a Dulbecco's Modified Eagle's medium containing 10% fetal bovine serum (FBS), 1% penicillin and amphotericin B. For fluorescence imaging, the cells were seeded in 24-well plates at  $1 \times 10^3/\text{mL}$ . After the cells were completely adherent, the medium was discarded. Fresh medium with 5 or 20  $\mu\text{L}$  of Rosup was added to the cells to culture for twenty minutes, and the supernatant was discarded. The cells were washed twice with cold PBS then treated with 50  $\mu\text{L}$  of mixed micelles (1 mg/mL loaded with 1  $\mu\text{g}/\text{mL}$  Nile Red) for 2 hours, then the original medium was discarded. The cells were washed 3 times with cold PBS, followed by using 4% paraformaldehyde to fix for 15 minutes. The fluorescence was immediately observed under a laser confocal microscope (Leica, TSC SP8). Green channel of dansyl was recorded at 500–520 nm with excitation at 340 nm. Red channel of Nile Red was at 620–640 nm with excitation at 560 nm. The Quantitative analysis of the fluorescence intensities from confocal laser microscopic images was performed using software imageJ (version: 1.53c).

## In vivo Imaging Studies

All in vivo experiments were performed in compliance with Third Military Medical University Animal Study Committee's requirements for the care and use of laboratory animals in research (Approval code: SYXK-PLA-20120031). 20 male nude mice (16–18 g) purchased from the Animal Experimentation Center of Third Military Medical University were used for the animal imaging study.

The mice were divided into four groups to establish an acute abdominal inflammation model: the first group was untreated as a control group; the second group was given an intraperitoneal (i.p.) injection of 400  $\mu$ L of saline; the third group was given an i.p. injection of 100  $\mu$ M Tiron in 400  $\mu$ L of saline; and the last group was given an i.p. injection of 0.2mg lipopolysaccharide endotoxin (LPS) in 400  $\mu$ L of saline. After 8 h, 200  $\mu$ L of mixed micelles were injected by i.p. to all 4 groups of mice. The animals were imaged as quadruplets after 30min using an IVIS Spectrum (Carestream Health, Canada) in fluorescence mode (excitation: 340 nm, emission: 520 nm).

## Statistical Analysis

Data were presented as mean  $\pm$  standard deviation (SD). Statistical significance of the differences between treatments was evaluated by ANOVA analysis and 2-tailed hypothesis testing was used for multiple groups. It was considered to be significant when  $p < 0.05$  (\*) and very significant when  $p < 0.005$  (\*\*).

## Results and Discussion

### Synthesis and Characterizations of Polymers

DAN-PPS-mPEG and DAB-PPS-mPEG were synthesized according to a synthesis route shown in Figure 1. The PPS block was firstly polymerized using a previously reported method of living anionic polymerization, followed by the endcapping of a hydrophilic mPEG-2k block.<sup>22</sup> The dansyl or dabsyl groups were conjugated to the hydrophobic block of the synthesized PPS-mPEG polymer as the fluorescent donor or quencher, respectively. The <sup>1</sup>H-NMR spectra confirmed the successful conjugation of the dansyl and dabsyl groups and that the degree of the polymerization of the PPS block is roughly 8 (Figure 2A and B, Table S1). GPC measurement of the synthesized polymers showed distinct peaks for each polymer and relatively narrow distributions (Figure 2C and Table S1).

### Micelle Preparation and Characterizations

A previously reported phase separation method was employed to prepare the DAN/DAB-PPS-mPEG mixed micelle dispersion.<sup>21</sup> Organic solvent THF was used to dissolve the mixed polymers and the organic solution was injected into the aqueous solution using as the continuous phase, followed by removing the organic solvent in a vacuum to obtain the micellar dispersion. The typical size of the prepared blank micelles (DAN:DAB= 1:3) was measured to be around 43.6 nm (Figure 3A). Moreover, Nile Red was used as a model drug to be encapsulated as well as a representative dye in this study. Nile Red loaded mixed micelles showed similar size with a slightly bigger averaged diameter at 48.3 nm

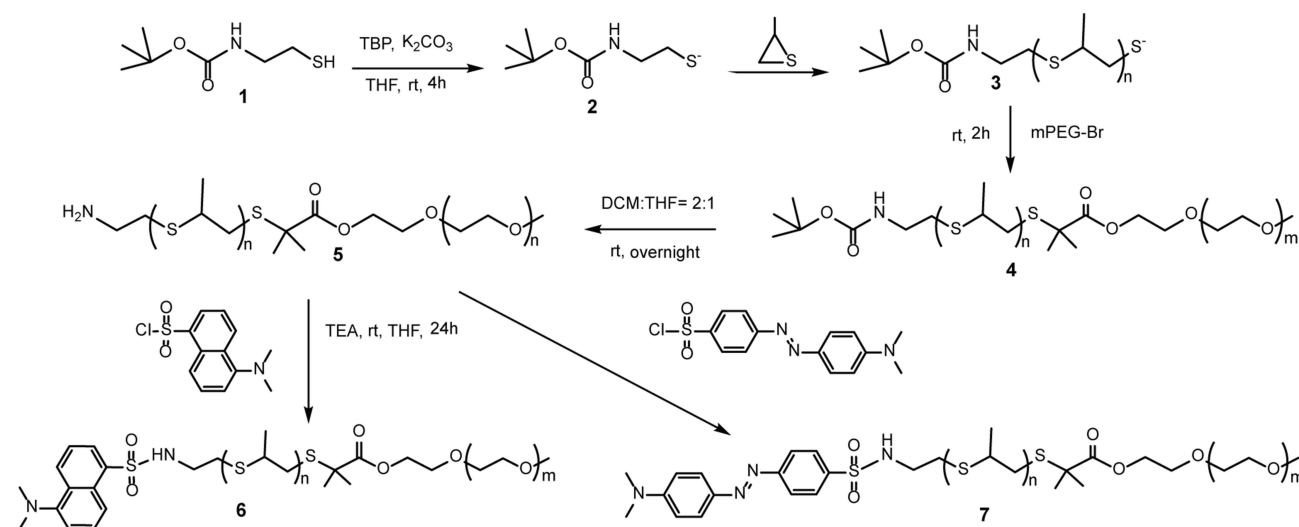


**Figure 1** Synthesis scheme of DAN/DAB-PPS-mPEG block copolymers.



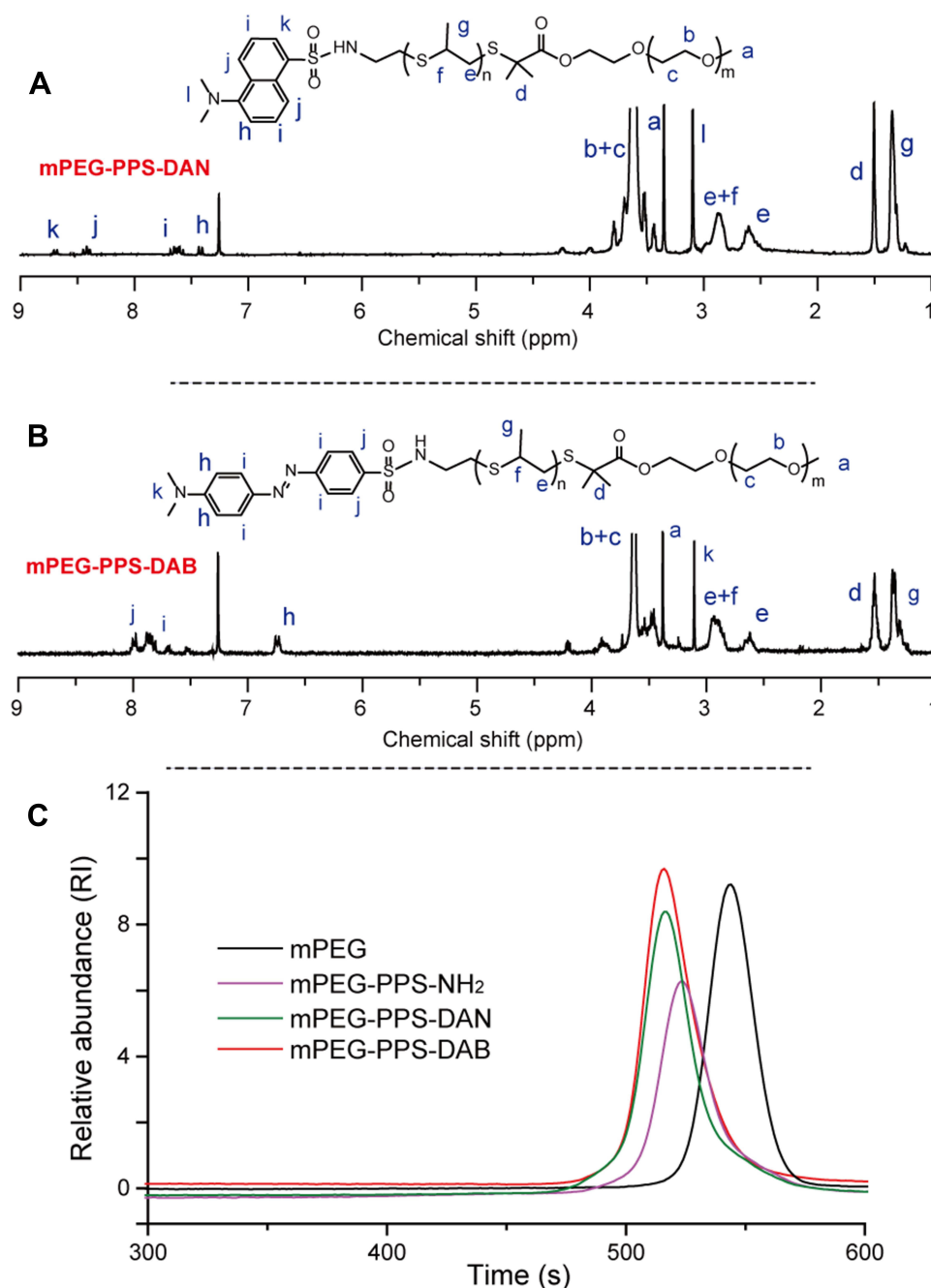


**Figure 2** Characterizations of synthesized polymers. (A) <sup>1</sup>H-NMR spectrum and peak assignments of DAN-PPS-mPEG, (B) <sup>1</sup>H-NMR spectrum and peak assignments of DAB-PPS-mPEG, (C) GPC traces of synthesized polymers.

(Figure 3A). The morphological features of the prepared blank and Nile Red loaded micelles observed by SEM showed relatively uniform distributions and spherical shapes of the particles (Figure 3A and B).

### Fluorescence Property of DAN/DAB-PPS-mPEG Mixed Micelles

The fluorescence property of the prepared DAN/DAB-PPS-mPEG mixed micelles were measured. Different ratios of DAN-PPS-mPEG to DAB-PPS-mPEG polymers were used to prepare mixed micelles. After testing their fluorescence spectra, the results showed that higher ratio of DAB-PPS-mPEG can better quench the fluorescence of dansyl groups (Figure S1). When the molar ratio of DAN-PPS-mPEG:DAB-PPS-mPEG reached to 1:3 or 1:4, the total fluorescence of

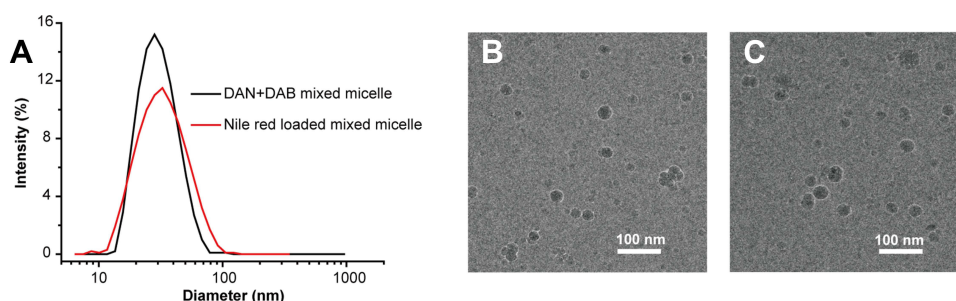


**Figure 3** The characterizations of DAN/DAB-PPS-mPEG mixed micelles. **(A)** The size distributions of DAN/DAB-PPS-mPEG mixed micelles and Nile Red loaded mixed micelles; **(B)** The SEM graph of DAN/DAB-PPS-mPEG mixed micelles; **(C)** The SEM graph of Nile Red loaded mixed micelles.

the micellar dispersion was mostly quenched, due to the higher amount of quencher (dansyl group) surrounded and quenched the fluorescent donor group. It was also found that encapsulating Nile Red into the pure DAN-PPS-mPEG micelle or mixed micelle did not influence the fluorescence of the dansyl groups ([Figure S1](#), dashed lines).

To test the possible self-quenching effect of the dansyl fluorophore in the micelles, DAN-PPS-mPEG micelles mixed with different amount of NH<sub>2</sub>-PPS-mPEG (1 mg/mL) were prepared. Their fluorescence intensities were measured and showed an increasing trend corresponding to higher amounts of DAN-PPS-mPEG in the micelles ([Figure S2](#)). DAN-PPS-mPEG micelles showed roughly 2.5 times higher fluorescence intensity compared to the mixed micelle sample containing only 25% dansyl fluorophores. The result suggested a certain degree of self-quenching effect may exist in the micelle sample containing higher concentrations of dansyl group, although this phenomenon can be greatly avoided by reducing the amount of dansyl groups in the micelles.

## Oxidation-Responsiveness of DAN/DAB-PPS-mPEG Mixed Micelles

The responsiveness of the mixed micelles to the oxidants was tested by fluorescence and dynamic light scattering (DLS) analysis. The fluorescent spectra of the sample upon oxidation changed at different time point. [Figure 4A](#) shows that the fluorescent intensity of the emission spectra of dansyl groups were gradually increased. With the oxidation of the PPS block in the core of the micelle, the change of the hydrophilicity of the polymer caused the decomposition of the micelles and accordingly, increased the distance between the dansyl and dabsyl groups and released the quenched fluorescence of dansyl groups. Furthermore, we introduced Nile Red as a model hydrophobic drug to understand the mechanism of drug release from the mixed micelle upon oxidation. Nile Red is a solvatochromic hydrophobic fluorescent dye which fluorescence is greatly compromised in polar environment, making it an ideal model drug to show its surrounding environment and in this study, illustrate the drug release and the integrity of the hydrophobic core of the micelles. As shown in [Figure 4B](#), the emission fluorescence intensity of Nile Red at 638 nm gradually decreased when the micelles was exposing to the oxidants, indicating that more and more Nile Red molecules were exposed in polar environment, resulted from the oxidation of the hydrophobic core of the micelles.

After exposing the Nile Red loaded micelles (DAN/DAB=1:3) in 0.5% H<sub>2</sub>O<sub>2</sub> solution, the scattering intensity of the micellar dispersion started to change ([Figure 4C](#)). The intensity increased slightly at first 30 minutes and decreased continuously in the next 10 hour until reaching very low levels. Since the scattering intensities reflect the hydrodynamic volumes of the particles in the system, this trend can be explained as that at the initial stage of oxidation, the micelles swelled due to the transformation of the thiol ether bonds to sulfoxide or sulfone groups in the PPS core, and the increased binding water molecules to the polymer chains. With the complete transformation by oxidation, the oxidized micelles eventually lost the capability of self-assembling and decomposed, showing decreasing scattering intensity in the system. [Figure 4D](#) summarizes the changes of the emissive fluorescence intensities of dansyl and Nile Red, as well as the scattering intensities of the sample. At the beginning of the oxidation, most of the micelles started to swell but not decompose, therefore the scattering intensity was increasing at the first 30 minutes and decreasing afterwards. The change of Nile Red was slightly quicker than that of dansyl at the beginning, possibly due to the infused water molecules partially quenched the Nile Red although the micelle was still not decomposed. Overall, the change of the fluorescence or

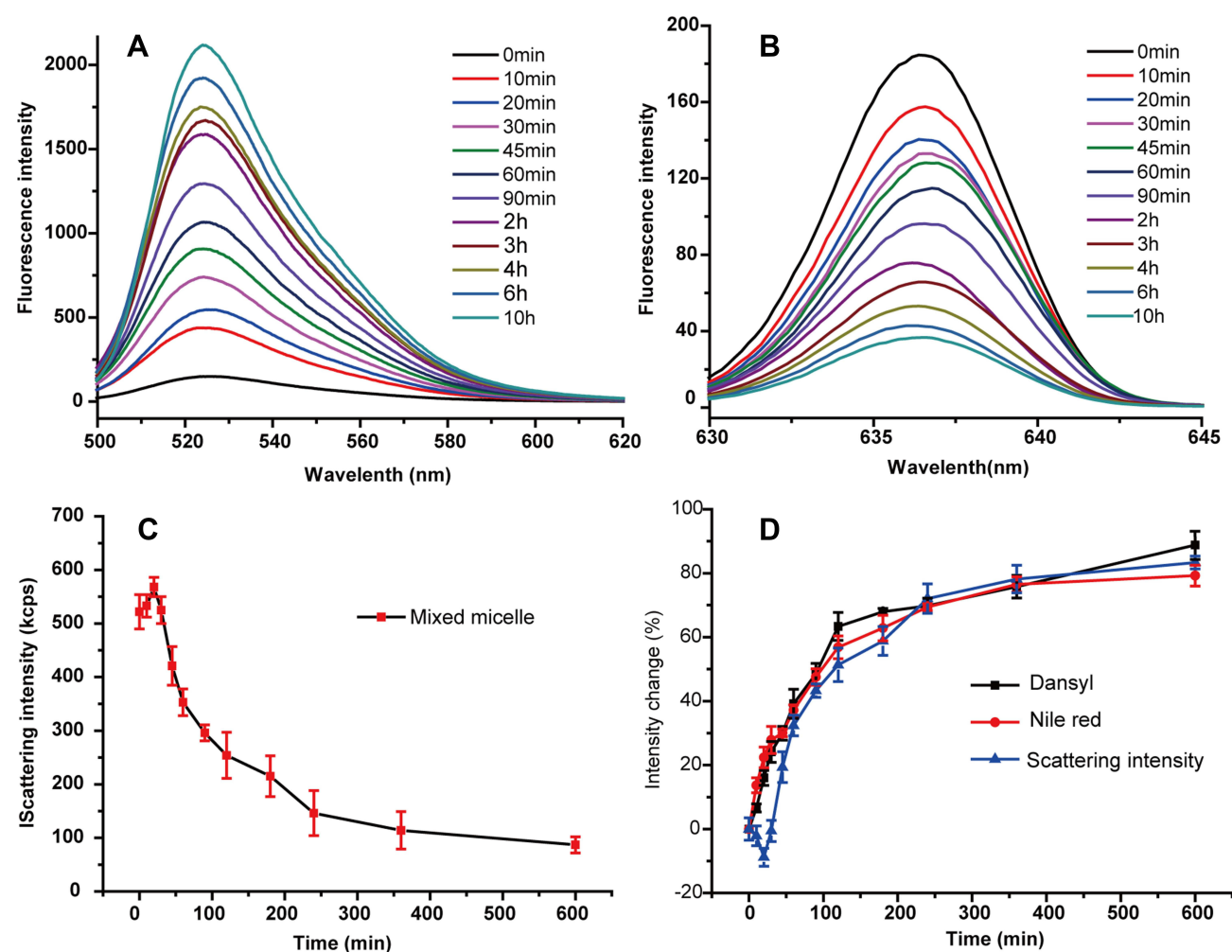


**Figure 4** The characterizations of DAN/DAB-PPS-mPEG mixed micelles. (A) Fluorescent emission spectrum of mixed micelles (excitation at 335 nm); (B) Fluorescent emission spectrum of mixed micelles (excitation at 560 nm); (C) The change of the scattering intensities of the micelles upon oxidation; (D) The percentage change of dansyl and Nile Red fluorescence and scattering intensities upon oxidation.

scattering intensities showed quite similar trends. In general, they had a phase of fast reaction/release and reached plateau around 4 h, followed by a phase of slow reaction/release. The results suggested that these three markers conformed to each other at great extents. In another word, the change of the scattering intensities, or the fluorescence of dansyl, can be used to estimate the release of Nile Red, or another encapsulated hydrophobic drug.

Untargeted disassembly and immature cargo leakage would weaken the delivery and diagnosis efficacy of the micelles, therefore the physiological stability of mixed micelles incubated in different media was tested (Figure S3). Compared to the samples in the 0.5%  $H_2O_2$  solution as a positive control, the scattering intensities of the micelles in rat plasma decreased 28% after 24 h incubation, possibly due to the dissociation caused by the reaction with the biological components in the plasma. On the other hand, the mixed micelles were very robust in water and PBS buffer solution, showing nearly constant scattering intensities during the 24 h incubation.

## Mixed Micelles for in vitro Cell Imaging

The restoration of the fluorescence of dansyl upon oxidation endows the micelle the capability to visualize the oxidants such as ROS. A stimulated cell model was used to confirm the fluorescence change of the DAN/DAB-PPS-mPEG mixed micelle and its visualization of ROS in vitro. The fibroblast cell line (L929) was selected as it serves as a major type of cells in the skin, while it can be stimulated by LPS to produce massive amount of ROS, which makes it an ideal model to study the injured skin tissue.<sup>25</sup> L929 cells were incubated with normal cell culture medium or with the addition of



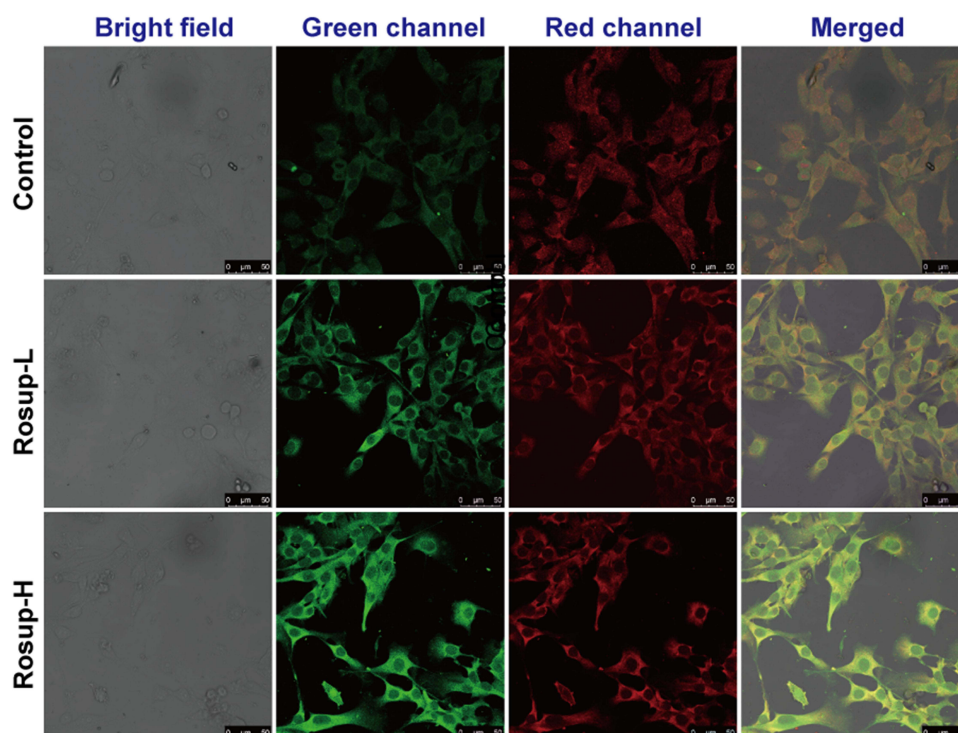


**Figure 5** Confocal laser microscopic images of inflammatory fibroblast cell lines. (Control) Cells incubated with DAN/DAB-PPS-mPEG; (Rosup-L) cells incubated with Rosup (5  $\mu$ M) and DAN/DAB-PPS-mPEG mixed micelles; (Rosup-H) cells incubated with Rosup (20  $\mu$ M) and DAN/DAB-PPS-mPEG mixed micelles. Green channel showed the fluorescence of dansyl group and red channel showed the fluorescence of Nile Red.

Rosup, a reagent to stimulate the production of intracellular ROS. In [Figure 5](#), after 2 h incubation, cells in control group showed weak green fluorescence of dansyl, suggesting the mostly quenched dansyl groups and the integrity of most mixed micelles. On the contrary, in both Rosup groups, the cells showed substantial green fluorescence after 2 h incubation, especially for the group of high dose of Rosup, suggesting the release of fluorescence from the dansyl groups due to the intracellular oxidation. A semi-quantitative analysis based on the data of the confocal laser microscopy experiment was performed and showed that the fluorescence intensities of ROS-L and ROS-H groups are 1.9 and 2.8 folds to that of the control group ([Figure S4](#)). The fluorescence of the Nile Red of the samples was also measured. Rosup groups and Control group all showed rather similar fluorescent intensities as the released Nile Red molecules may bind to the intracellular lipophilic components such as lipid drops or lipid rafts, and emitted red fluorescence upon excitation. The results also showed that encapsulating Nile Red to reflect the intracellular oxidation of the micelles was impractical, as the intracellular fluorescence of Nile Red was not greatly influenced before and after its release from the micelle.

## In vivo Imaging of Mice with Mixed Micelles

To assess the potential of DAN/DAB-PPS-mPEG micelles for bioimaging in living animals, we studied whether they can be utilized for fluorescence imaging in an abdominal inflammation model of mouse. Localized injection of LPS can cause acute inflammatory reactions in the injected sites and induce massive production of ROS. As shown in [Figure 6](#), comparing to the control group, the LPS group showed obvious fluorescence at the abdominal site. This is due to the extensively existed ROS in the inflammatory site triggered the oxidation and the decomposition of the micelles, and correspondingly, the restored fluorescence of dansyl upon excitation. This reaction can be inhibited by the addition of Tiron, which is a reducing agent to counteract the inflammatory reactions. The Tiron group showed negligible fluorescence, only account for 7% to that of the LPS group ([Figure 6B](#)). Saline group show substantial fluorescence (38% of LPS group) as saline caused certain degree of inflammatory reactions when injected to the abdomen. The results confirmed the suitability of using DAN/DAB-PPS-mPEG micelles to image the inflammatory reactions in vivo.

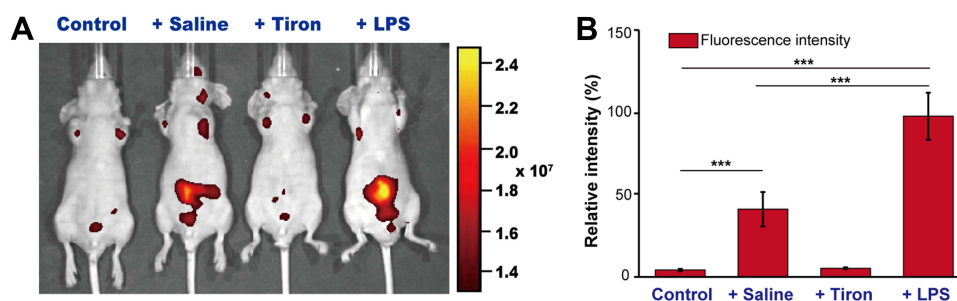


**Figure 6** In vivo imaging of the inflammatory reactions using DAN/DAB-PPS-mPEG mixed micelles. **(A)** control: a mouse without surgery before administration of mixed micelles; Saline: a mouse pre-injected with saline before administration of mixed micelles; Tiron: a mouse pre-injected with Tiron before administration of mixed micelles; LPS: a mouse pre-injected with LPS before administration of mixed micelles; **(B)** statistical analysis of the fluorescence intensity of the four groups (n=5). It was considered to be very significant when  $p < 0.005$  (\*\*\*).

Moreover, based on the in vitro experiment, DAN/DAB-PPS-mPEG micelles have the potential to reflect the extent of encapsulated drug release upon oxidation, which will greatly aid the visualization of the release of non-fluorescent drugs.

## Conclusion

In this study, DAN/DAB-PPS-mPEG polymers were synthesized and their mixed micelles were prepared. The micelles demonstrated oxidation-responsive behaviors and morphological changes with altered fluorescence spectra based on the on-off FRET effect. The results confirmed the oxidants can trigger the oxidation of the core of the micelles and lead to the decomposition of the particulate structure and restored fluorescence of dansyl groups. Based on this mechanism, the mixed micelles were incubated with inflammatory fibroblast cells and showed dose-dependent fluorescent restoration. Furthermore, using the mixed micelles in an in vivo acute inflammatory reaction model, the micelles showed its ability to visualize the inflammatory site in the abdomen of the mice. The results confirmed that DAN/DAB-PPS-mPEG mixed micelles can respond to ROS and release encapsulated cargos with corresponding fluorescence restoration, and visualize the inflammatory cells in vitro and inflammatory reactions in vivo. This novel oxidation-responsive nanocarrier with the ability of visualizing ROS possesses huge potential to be used to treat different human diseases related with acute or chronic inflammation, such as rheumatoid arthritis and cancers.

## Supporting Information

More characterization and fluorescence data are supplied as [Supplementary Information](#).

## Acknowledgments

This work was supported by the National Natural Science Foundation of China (No. 82071367), Science and Technology Program of Guangzhou, China (No. 202102080458).

## Disclosure

The authors declare no conflicts of interest in this work.

## References

1. Sies H, Jones DP. Reactive oxygen species (ROS) as pleiotropic physiological signalling agents. *Nat Rev Mol Cell Biol.* 2020;21(7):363–383. doi:10.1038/s41580-020-0230-3
2. Forrester SJ, Kikuchi DS, Hernandez MS, Xu Q, Griendling KK. Reactive oxygen species in metabolic and inflammatory signaling. *Circ Res.* 2018;122(6):877–+. doi:10.1161/CIRCRESAHA.117.311401
3. Yu Q, Lu Z, Tao L, et al. ROS-dependent neuroprotective effects of NaHS in ischemia brain injury involves the PARP/AIF pathway. *Cell Physiol Biochem.* 2015;36(4):1539–1551. doi:10.1159/000430317
4. Rhee SG. Redox signaling: hydrogen peroxide as intracellular messenger. *Exp Mol Med.* 1999;31(2):53–59. doi:10.1038/emmm.1999.9
5. Singh A, Kukreti R, Saso L, Kukreti S. Oxidative stress: a key modulator in neurodegenerative diseases. *Molecules.* 2019;24(8):1583. doi:10.3390/molecules24081583

6. Oliveira Volpe CM, Villar-Delfino PH, Ferreira Dos Anjos PM, Nogueira-Machado JA. Cellular death, reactive oxygen species (ROS) and diabetic complications. *Cell Death Dis.* **2018**;9:1–9.
7. Srinivas US, Tan BWQ, Vellayappan BA, Jeyasekharan AD. ROS and the DNA damage response in cancer. *Redox Biol.* **2019**;25:101084. doi:10.1016/j.redox.2018.101084
8. Yang B, Chen Y, Shi J. Reactive Oxygen Species (ROS)-based nanomedicine. *Chem Rev.* **2019**;119(8):4881–4985. doi:10.1021/acs.chemrev.8b00626
9. Sharma A, Arambula JF, Koo S, et al. Hypoxia-targeted drug delivery. *Chem Soc Rev.* **2019**;48(3):771–813. doi:10.1039/c8cs00304a
10. Joshi-Barr S, Lux CD, Mahmoud E, Almutairi A. Exploiting oxidative microenvironments in the body as triggers for drug delivery systems. *Antioxid Redox Signal.* **2014**;21(5):730–754. doi:10.1089/ars.2013.5754
11. Rahdar A, Hajinezhad MR, Sargazi S, et al. Biochemical effects of deferasirox and deferasirox-loaded nanomicelles in iron-intoxicated rats. *Life Sci.* **2021**;270:119146. doi:10.1016/j.lfs.2021.119146
12. Napoli A, Valentini M, Tirelli N, Muller M, Hubbell JA. Oxidation-responsive polymeric vesicles. *Nat Mater.* **2004**;3(3):183–189. doi:10.1038/nmat1081
13. Lallana E, Tirelli N. Oxidation-responsive polymers: which groups to use, how to make them, what to expect from them (biomedical applications). *Macromol Chem Phys.* **2013**;214(2):143–158. doi:10.1002/macp.201200502
14. Ma N, Li Y, Ren H, Xu H, Li Z, Zhang X. Selenium-containing block copolymers and their oxidation-responsive aggregates. *Polym Chem.* **2010**;1(10):1609–1614. doi:10.1039/c0py00144a
15. Ding Y, Yi Y, Xu H, Wang Z, Zhang X. Redox-responsive thermal sensitivity based on a selenium-containing small molecule. *Chem Commun.* **2014**;50(20):2585–2588. doi:10.1039/c3cc49753d
16. Chen X, Wang F, Hyun JY, et al. Recent progress in the development of fluorescent, luminescent and colorimetric probes for detection of reactive oxygen and nitrogen species. *Chem Soc Rev.* **2016**;45(10):2976–3016. doi:10.1039/C6CS00192K
17. Lou Z, Li P, Han K. Redox-responsive fluorescent probes with different design strategies. *Acc Chem Res.* **2015**;48(5):1358–1368. doi:10.1021/acs.accounts.5b00009
18. Cash TP, Pan Y, Simon MC. Reactive oxygen species and cellular oxygen sensing. *Free Radic Biol Med.* **2007**;43(9):1219–1225. doi:10.1016/j.freeradbiomed.2007.07.001
19. Zheng Q, He Y, Tang Q, et al. An NIR-guided aggregative and self-immolative nanosystem for efficient cancer targeting and combination anticancer therapy. *Mol Pharm.* **2018**;15(11):4985–4994. doi:10.1021/acs.molpharmaceut.8b00599
20. Tang M, Hu P, Zheng Q, et al. Polymeric micelles with dual thermal and reactive oxygen species (ROS)-responsiveness for inflammatory cancer cell delivery. *J Nanobiotechnology.* **2017**;15. doi:10.1186/s12951-017-0275-4
21. Hu P, Tirelli N. Scavenging ROS: superoxide dismutase/catalase mimetics by the use of an oxidation-sensitive nanocarrier/enzyme conjugate. *Bioconjug Chem.* **2012**;23(3):438–449. doi:10.1021/bc200449k
22. Hu P, Tirelli N. Inter-micellar dynamics in block copolymer micelles: FRET experiments of macroamphiphile and payload exchange. *React Funct Polym.* **2011**;71(3):303–314. doi:10.1016/j.reactfunctpolym.2010.10.010
23. Park S-H, Kwon N, Lee J-H, Yoon J, Shin I. Synthetic ratiometric fluorescent probes for detection of ions. *Chem Soc Rev.* **2020**;49(1):143–179. doi:10.1039/C9CS00243J
24. Wu L, Huang C, Emery BP, et al. Forster resonance energy transfer (FRET)-based small-molecule sensors and imaging agents. *Chem Soc Rev.* **2020**;49(15):5110–5139. doi:10.1039/C9CS00318E
25. Wang L, Song D, Wei C, et al. Telocytes inhibited inflammatory factor expression and enhanced cell migration in LPS-induced skin wound healing models in vitro and in vivo. *J Transl Med.* **2020**;18(1):1–4.

## International Journal of Nanomedicine

Dovepress

### Publish your work in this journal

The International Journal of Nanomedicine is an international, peer-reviewed journal focusing on the application of nanotechnology in diagnostics, therapeutics, and drug delivery systems throughout the biomedical field. This journal is indexed on PubMed Central, MedLine, CAS, SciSearch®, Current Contents®/Clinical Medicine, Journal Citation Reports/Science Edition, EMBase, Scopus and the Elsevier Bibliographic databases. The manuscript management system is completely online and includes a very quick and fair peer-review system, which is all easy to use. Visit <http://www.dovepress.com/testimonials.php> to read real quotes from published authors.

Submit your manuscript here: <https://www.dovepress.com/international-journal-of-nanomedicine-journal>